J|A|C|S ARTICLES

Published on Web 12/15/2010

Topochemical Synthesis of Co−Fe Layered Double Hydroxides at Varied Fe/Co Ratios: Unique Intercalation of Triiodide and Its Profound Effect

Renzhi Ma,* Jianbo Liang, Kazunori Takada, and Takayoshi Sasaki

International Center for Materials Nanoarchitectonics, National Institute for Materials Science, 1-1 Namiki, Tsukuba, Ibaraki 305-0044, Japan

Received September 28, 2010; E-mail: MA.Renzhi@nims.go.jp

Abstract: Co−Fe layered double hydroxides at different Fe/Co ratios were synthesized from brucite-like $Co^{2+}_{1-x}Fe^{2+}_{x}(OH)_2$ ($0 \le x \le 1/3$) via oxidative intercalation reaction using an excess amount of iodine as the oxidizing agent. A new redoxable species: triiodide (I_3^-), promoted the formation of single-phase Co−Fe LDHs. The results point to a general principle that LDHs with a characteristic ratio of total trivalent and divalent cations (M^{3+}/M^{2+}) at 1/2 may be the most stable in the oxidative intercalation procedure. At low Fe content, e.g., starting from $Co^{2+}_{1-x}Fe^{2+}_{x}(OH)_2$ ($x < 1/3$), partial oxidation of Co^{2+} to Co^{3+} takes place to reach the M^{3+}/M^{2+} threshold of 1/2 in as-transformed $Co^{2+}_{2/3}-(Co^{3+}_{1/3-x}-Fe^{3+}_{x})$ LDHs. Also discovered was the cointercalation of triiodide and iodide into the interlayer gallery of as-transformed LDH phase, which profoundly impacted the relative intensity ratio of basal Bragg peaks as a consequence of the significant X-ray scattering power of triiodide. In combination with XRD simulation, the LDH structure model was constructed by considering both the host layer composition/charge and the arrangement of interlayer triiodide/iodide. The work provides a clear understanding of the thermodynamic and kinetic factors associated with the oxidative intercalation reaction and is helpful in elucidating the formation of LDH structure in general.

Introduction

Layered double hydroxides (LDHs) with a general formula of $[M^{2+}_{1-x}M^{3+}_{x}(OH)_2]^{x+}[A^{n-}_{x/n}\cdot mH_2O]^{x-}$ (M^{2+} and M^{3+} are divalent and trivalent metal cations, respectively; A^{n-} is the charge-balancing anion of valence n; $x = M^{3+}/(M^{2+} + M^{3+})$ ($1/5 \le x \le 1/3$)), hold special importance as a rare anion-exchangeable layered host in materials chemistry as well as afford multifunctionality such as for adsorbents, catalysts, solid state nanoreactors, molecular sieves, polymer composites, bioactive materials, and pharmaceuticals.[1−5] Recently, it was demonstrated that LDH crystallites can be exfoliated into ultimate two-dimensional nanosheets through soft-chemical treatment.[6−9] The positively charged LDH nanosheets are regarded as ideal building blocks to fabricate ultrathin films and diverse nanoarchitectures due to their unilamellar thickness. Among LDHs, the $M^{2+}-Al^{3+}$ category ($M^{2+} = Mg^{2+}$, Fe^{2+}, Co^{2+}, Ni^{2+}, Zn^{2+}, etc.) has been extensively studied, due in part to the facts that samples with reasonable crystallinity can be routinely prepared via coprecipitation,[1,2] or more recently, that

(1) (a) Allmann, R. *Acta Crystallogr.* **1968**, *B24*, 972. (b) Miyata, S.; Okada, A. *Clays Clay Miner.* **1977**, *25*, 14. (c) Miyata, S. *Clays Clay Miner.* **1983**, *31*, 305. (d) Clearfield, A. *Chem. Rev.* **1988**, *88*, 125. (e) Braterman, P. S.; Xu, Z. P.; Yarberry, F. In Layered Double Hydroxides (LDHs). *Handbook of Layered Materials*; Auerbach, S. M., Carrado, K. A., Dutta, P. K., Eds.; Marcel Dekker, Inc.: New York, NY, U.S., 2004.

(2) (a) Bish, D. L. *Bull. Mineral.* **1980**, *103*, 170. (b) Bonnet, S.; Forano, C.; de Roy, A.; Besse, J. P.; Maillard, P.; Momenteau, M. *Chem. Mater.* **1996**, *8*, 1962. (c) Pavan, P. C.; Gomes, G. de A.; Valim, J. B. *Microporous Mesoporous Mater.* **1998**, *21*, 659. (d) Tronto, J.; Sanchez, K. C.; Crepaldi, E. L.; Naal, Z.; Klein, S. I.; Valim, J. B. *J. Phys. Chem. Solid* **2004**, *65*, 493. (e) Pérez, M. R.; Pavlovic, I.; Barriga, C.; Cornejo, J.; Hermosín, M. C.; Ulibarri, M. A. *Appl. Clay Sci.* **2006**, *32*, 245.

(3) (a) Leroux, F.; Besse, J.-P. *Chem. Mater.* **2001**, *13*, 3507. (b) Darder, M.; López-Blanco, M.; Aranda, P.; Leroux, F.; Ruiz-Hitzky, E. *Chem. Mater.* **2005**, *17*, 1969. (c) Desigaux, L.; Belkacem, M. B.; Richard, P.; Cellier, J.; Léone, P.; Cario, L.; Leroux, F.; Taviot-Guého, C.; Pitard, B. *Nano Lett.* **2006**, *6*, 199. (d) Ma, S.; Fan, C.; Du, L.; Huang, G.; Yang, X.; Tang, W.; Makita, Y.; Ooi, K. *Chem. Mater.* **2009**, *21*, 3602.

(4) (a) Cavani, F.; Trifirò, F.; Vaccari, A. *Catal. Today* **1991**, *11*, 173. (b) McKenzie, A. L.; Fishel, C. T.; Davis, R. J. *J. Catal.* **1992**, *138*, 547. (c) Sels, B.; De Vos, D.; Buntinx, M.; Pierard, F.; Kirsch-De Mesmaeker, A.; Jacobs, P. *Nature* **1999**, *400*, 855. (d) Sels, B. F.; De Vos, D. E.; Jacobs, P. A. *Catal. Rev. Sci. & Eng.* **2001**, *43*, 443. (e) Li, F.; Tan, Q.; Evans, D. G.; Duan, X. *Catal. Lett.* **2005**, *99*, 151.

(5) (a) Choy, J.-H.; Kwak, S.-Y.; Park, J.-S.; Jeong, Y.-J.; Portier, J. *J. Am. Chem. Soc.* **1999**, *121*, 1399. (b) Choy, J.-H.; Kwak, S.-Y.; Jung, Y.-J.; Park, J.-S. *Angew. Chem., Int. Ed.* **2000**, *39*, 4042. (c) Oh, J.-M.; Biswick, T. T.; Choy, J.-H. *J. Mater. Chem.* **2009**, *19*, 2553. (d) Sasaki, S.; Aisawa, S.; Hirahara, H.; Sasaki, A.; Nakayama, H.; Narita, E. *J. Solid State Chem.* **2006**, *179*, 1129. (e) Sasaki, S.; Aisawa, S.; Hirahara, H.; Sasaki, A.; Nakayama, H.; Narita, E. *J. Eur. Ceram. Soc.* **2006**, *26*, 655.

(6) (a) Adachi-Pagano, M.; Forano, C.; Besse, J.-P. *Chem. Commun.* **2000**, 91. (b) Leroux, F.; Adachi-Pagano, M.; Intissar, M.; Chauvière, S.; Forano, C.; Besse, J.-P. *J. Mater. Chem.* **2001**, *11*, 105. (c) O'Leary, S.; O'Hare, D.; Seeley, G. *Chem. Commun.* **2002**, 1506. (d) Chen, W.; Feng, L.; Qu, B. *Chem. Mater.* **2004**, *16*, 368. (e) Jobbágy, M.; Regazzoni, A. E. *J. Colloid Interface Sci.* **2004**, *275*, 345. (f) Venugopal, B. R.; Shivakumara, C.; Rajamathi, M. *J. Colloid Interface Sci.* **2006**, *294*, 234.

(7) (a) Hibino, T.; Jones, W. *J. Mater. Chem.* **2001**, *11*, 1321. (b) Hibino, T. *Chem. Mater.* **2004**, *16*, 5482. (c) Guo, Y.; Zhang, H.; Zhao, L.; Li, G. D.; Chen, J. S.; Xu, L. *J. Solid State Chem.* **2005**, *178*, 1830. (d) Wu, Q.; Olfsen, A.; Vistad, Ø. B.; Roots, J.; Norby, P. *J. Mater. Chem.* **2005**, *15*, 4695. (e) Okamoto, K.; Sasaki, T.; Fujita, T.; Iyi, N. *J. Mater. Chem.* **2006**, *16*, 1608.

(8) (a) Hibino, T.; Kobayashi, M. *J. Mater. Chem.* **2005**, *15*, 653. (b) Iyi, N.; Ebina, Y.; Sasaki, T. *Langmuir* **2008**, *24*, 5591.

well-developed hexagonal microplatelet crystallites were prepared via so-called homogeneous precipitation.[9−11] As homogeneous precipitation must utilize the amphoteric feature of Al^{3+} during hydroxide crystallization, high-quality LDH samples with non-Al^{3+} host layer composition are difficult to realize and thus less explored. LDHs comprising all transition-metal elements with redox potential (e.g., Fe, Co, Ni) are expected to have, in addition to general $M^{2+}-Al^{3+}$ derived functionalities, more interesting features for electronic, magnetic, and electrochemical applications.

Very recently, we demonstrated an innovative topochemical synthetic method, namely oxidative intercalation whereby $Co^{2+}_{2/3}-Fe^{3+}_{1/3}$, $Co^{2+}_{2/3}-Co^{3+}_{1/3}$ and $(Co^{2+}_{1-3x/2}-Ni^{2+}_{3x/2})_{2/3}-Co^{3+}_{1/3}$ ($0 \le x \le 1/2$) LDHs were transformed from corresponding brucite-like hydroxides ($M^{2+}(OH)_2$) such as $Co^{2+}_{2/3}Fe^{2+}_{1/3}(OH)_2$, $Co^{2+}(OH)_2$, and $Co^{2+}_{1-x}Ni^{2+}_{x}(OH)_2$, respectively, employing either iodine (I_2) or bromine (Br_2) as the oxidizing agent in suitable organic solvents.[12−14] LDH products thus obtained retain the hexagonal microplatelet morphology of starting brucite-like hydroxides and exhibit much higher quality than those prepared via conventional coprecipitation. Especially, all resultant LDHs have the same M^{3+}/M^{2+} ratio of 1/2, i.e., a host layer charge $M^{3+}/(M^{2+} + M^{3+})$ of 1/3, even though the elemental composition varies over a wide range ($M^{2+} = Co^{2+}$ in $Co^{2+}_{2/3}-Fe^{3+}_{1/3}$ and $Co^{2+}_{2/3}-Co^{3+}_{1/3}$, or Co^{2+}/Ni^{2+} for $(Co^{2+}_{1-3x/2}-Ni^{2+}_{3x/2})_{2/3}-Co^{3+}_{1/3}$ LDHs; $M^{3+} = Fe^{3+}$ for $Co^{2+}_{2/3}-Fe^{3+}_{1/3}$, or Co^{3+} for $Co^{2+}_{2/3}-Co^{3+}_{1/3}$ and $(Co^{2+}_{1-3x/2}-Ni^{2+}_{3x/2})_{2/3}-Co^{3+}_{1/3}$ LDHs.). These observations provide important insight into both thermodynamic and kinetic factors affecting the oxidative intercalation reaction.

From a thermodynamic point of view, the M^{3+}/M^{2+} ratio or the host layer charge $M^{3+}/(M^{2+} + M^{3+})$ would be affected by the interplay between the host layers and interlayer guests (here, the guests represent iodide (I^-) or bromide (Br^-) produced in situ). On the host layer part, a higher layer charge, attained by oxidizing more M^{2+} to M^{3+}, would be beneficial for stabilizing the LDH structure by enhanced electrostatic interaction between the positive host layers and anionic guests. Several studies indicate the LDH with a M^{3+}/M^{2+} ratio of 1/2, so that two M^{2+} and one M^{3+} are neatly ordered in a trigonal lattice, is preferable for achieving a high layer charge while avoiding direct nearest neighboring of M^{3+} (charge center).[15,16] On the anionic side, in situ I^- or Br^- accompanying the oxidation of M^{2+} to M^{3+} would occupy the gallery site near each M^{3+} cation to balance the positive charge locally. Charge balance and steric restriction might, in an ideal model, lead to an ordered array of I^- or Br^- that is commensurate with the cationic ordering in the host layer. The question arises as to whether or not a host layer composition with M^{3+}/M^{2+} ratio lower than 1/2 can be rationally achieved through the oxidative intercalation process. This affords the prospect of tuning the functionality of LDHs by varying M^{3+}/M^{2+} composition.

From a kinetic point of view, an abundant oxidizing agent and a long treatment period are considered beneficial in promoting and completing the oxidative conversion from brucite to LDH. Stoichiometric iodine appears sufficient in transforming $Co^{2+}_{2/3}Fe^{2+}_{1/3}(OH)_2$ into $Co^{2+}_{2/3}-Fe^{3+}_{1/3}$ LDH due to the easy oxidation tendency of Fe^{2+}.[12] On the other hand, the use of excess bromine is mandatory for the oxidation of Co^{2+} and conversion into $Co^{2+}_{2/3}-Co^{3+}_{1/3}$ and $(Co^{2+}_{1-3x/2}-Ni^{2+}_{3x/2})_{2/3}-Co^{3+}_{1/3}$ LDHs.[13,14] Accordingly, it is important to probe the oxidative intercalation reaction for $Co^{2+}_{1-x}Fe^{2+}_{x}(OH)_2$ under conditions employing an excess amount of iodine. This would be vital for fully understanding the kinetic factors associated with the reaction, especially for samples at Fe/Co ratio lower than 1/2.

In the current study, brucite-like $Co^{2+}_{1-x}Fe^{2+}_{x}(OH)_2$ at different Fe/Co ratios ($x = 0$, 1/5, 1/4, 1/3) were synthesized. The oxidative intercalation reaction was designed to convert the brucite into LDH, through the use of an excess amount or concentrated solution of iodine. The results revealed that, regardless of Fe/Co ratio, $Co^{2+}_{2/3}-(Co^{3+}_{1/3-x}-Fe^{3+}_{x})$ LDHs were found with the same M^{3+}/M^{2+} ratio of 1/2. More interestingly, a unique phenomenon, cointercalating triiodide (I_3^-) and iodide into the interlayer gallery of as-transformed LDHs, was discovered, which imparted an unusual change in the relative intensity ratio of basal Bragg reflections. Cointercalation of triiodide, which is seldom encountered in conventional anion-exchange procedures, offers a precious opportunity not only to reveal the kinetics associated with the oxidative intercalation reaction but also to understand the LDH structure in-depth regarding host layer composition and charge, interlayer anionic species, and steric distribution, etc.

Experimental Section

Synthesis of Brucite-Like $Co_{1-x}Fe_x(OH)_2$ ($x = 0$, 1/5, 1/4, 1/3). Highly crystalline hexagonal platelets of brucite-like Co−Fe hydroxides were synthesized via refluxing a dilute aqueous solution of divalent cobalt and/or ferrous cations with hexamethylenetetramine (HMT) under nitrogen gas protection.[12,13] Typically, cobalt chloride ($CoCl_2 \cdot 6H_2O$) and ferrous chloride ($FeCl_2 \cdot 4H_2O$) at different Fe/Co ratios, were dissolved by Milli-Q water in a 1000 cm^3 three-neck flask to prepare a total metal cation concentration of 7.5 mM. The flask was purged by nitrogen gas. An HMT solution of 50 cm^3 (1.2 M), sharing the same nitrogen purging route, was stored above one of the flask necks with a separating valve. After overnight purging, HMT solution was let into the flask by opening the separating valve, which did not allow any outside air/O_2 contamination. The mixed solution was then refluxed for ~5 h under continuous magnetic stirring. Pink-colored solid products were recovered by quickly filtering the precipitate in a glovebag filled with nitrogen, then washing several times with degassed Milli-Q

(9) (a) Li, L.; Ma, R.; Ebina, Y.; Iyi, N.; Sasaki, T. *Chem. Mater.* **2005**, *17*, 4386. (b) Liu, Z.; Ma, R.; Osada, M.; Iyi, N.; Ebina, Y.; Takada, K.; Sasaki, T. *J. Am. Chem. Soc.* **2006**, *128*, 4872. (c) Liu, Z.; Ma, R.; Ebina, Y.; Iyi, N.; Takada, K.; Sasaki, T. *Langmuir* **2007**, *23*, 861. (d) Ma, R.; Liu, Z.; Li, L.; Iyi, N.; Sasaki, T. *J. Mater. Chem.* **2006**, *16*, 3809.

(10) (a) Cai, H.; Hillier, A. C.; Franklin, K. R.; Nunn, C. C.; Ward, M. D. *Science* **1994**, *266*, 1551. (b) Costantino, U.; Marmottini, F.; Nocchetti, M.; Vivani, R. *Eur. J. Inorg. Chem.* **1998**, *10*, 1439. (c) Costantino, U.; Coletti, N.; Nocchetti, M.; Aloisi, G. G.; Elisei, F.; Latterini, L. *Langmuir* **2000**, *16*, 10351. (d) Ogawa, M.; Kaiho, H. *Langmuir* **2002**, *18*, 4240. (e) Oh, J.-M.; Hwang, S.-H.; Choy, J.-H. *Solid State Ionics* **2002**, *151*, 285. (f) Adachi-Pagano, M.; Forano, C.; Besse, J.-P. *J. Mater. Chem.* **2003**, *13*, 1988. (g) Sileo, E. E.; Jobbágy, M.; Paiva-Santos, C. O.; Regazzoni, A. E. *J. Phys. Chem. B* **2005**, *109*, 10137. (h) Rao, M. M.; Reddy, B. R.; Jayalakshmi, M.; Jaya, V. S.; Sridhar, B. *Mater. Res. Bull.* **2005**, *40*, 347.

(11) Iyi, N.; Matsumoto, T.; Kaneko, Y.; Kitamura, K. *Chem. Lett.* **2004**, *33*, 1122.

(12) Ma, R.; Liu, Z.; Takada, K.; Iyi, N.; Bando, Y.; Sasaki, T. *J. Am. Chem. Soc.* **2007**, *129*, 5257.

(13) Ma, R.; Takada, K.; Fukuda, K.; Iyi, N.; Bando, Y.; Sasaki, T. *Angew. Chem., Int. Ed.* **2008**, *47*, 86.

(14) Liang, J.; Ma, R.; Iyi, N.; Ebina, Y.; Takada, K.; Sasaki, T. *Chem. Mater.* **2010**, *22*, 371.

(15) Belloto, M.; Rebours, B.; Clause, O.; Lynch, J.; Elkaïm, E. *J. Phys. Chem.* **1996**, *100*, 8527.

(16) Sideris, P. J.; Nieslen, U. G.; Gan, Z. H.; Grey, C. P. *Science* **2008**, *321*, 113.

water and anhydrous ethanol. All the procedures were carried out under special care to avoid possible oxidation of ferrous cations by air/O_2.

Oxidative Intercalation Reaction. Oxidizing all ferrous cations in 1 mol $Co^{2+}_{1-x}Fe^{2+}_{x}(OH)_2$ theoretically requires $x/2$ mol of I_2. For the standard oxidative intercalation reaction to oxidize 1 mmol of $Co^{2+}_{1-x}Fe^{2+}_{x}(OH)_2$, nearly stoichiometric iodine (20% excess) matching the theoretically required amount was dissolved in 50 cm^3 chloroform ($CHCl_3$). On the other hand, a much larger amount of iodine (typically >10 × $x/2$ mol) was dissolved in chloroform for the excess treatment. As-prepared brucite-like $Co^{2+}_{1-x}Fe^{2+}_{x}(OH)_2$ was dispersed and magnetically stirred in the $I_2/CHCl_3$ solution at room temperature for about 1 day to 1 week. A darkish product was collected by filtering, and washing repeatedly with anhydrous ethanol until the filtrate appeared colorless.

Anion Exchange. After oxidative intercalation, the product was exchanged into other anionic forms via a previously reported ethanol-assisted anion-exchange procedure.[14] For example, a perchlorate (ClO_4^-) solution (1.5 M) was prepared by dissolving 0.3 mol of $NaClO_4$ into 200 cm^3 of ethanol−water binary liquid (1:1 v/v) in a flask. Iodine-treated sample (0.25 g) was dispersed into the solution after purging with nitrogen gas. The vessel was tightly capped and mechanically shaken for 24 h at room temperature. The exchanged product was filtered, washed with degassed Milli-Q water and anhydrous ethanol, and air-dried for further characterization.

Characterizations. X-ray diffraction (XRD) data were recorded by a Rigaku Rint-2200 diffractometer with monochromatic Cu Kα radiation (λ = 0.154 05 nm). XRD simulation was carried out by using the multipurpose pattern fitting program RIETAN-2000.[17] Morphologies and dimensions of the synthesized products were examined on a JEOL JSM-6700F field emission scanning electron microscope (FE-SEM). Transmission electron microscopy (TEM) was performed on a JEOL JEM-3100F energy-filtering transmission microscope. Elemental compositions of Co, Fe, and I were analyzed with an energy dispersive X-ray spectrometer (EDS). Thermogravimetric (TG) measurement was carried out using a Rigaku TGA-8120 instrument in a temperature range 25−1000 °C at a heating rate of 5 °C min^{-1} in air. With a dilute suspension in ethanol using a quartz cell with a path length of 10 mm, UV−vis absorption spectra were recorded on a Hitachi U-4100 spectrophotometer. X-ray photoelectron spectroscopy (XPS) spectra were recorded on a PHI XPS 5700 using Al Kα (200 W, 1486.6 eV). All spectra were calibrated using the C 1s peak and O 1s peak.

The ratio of divalent and trivalent metal cations in the sample was determined by chemical titration. Typically, about 0.030 g samples were dissolved in diluted HCl and separated into two equal portions. One portion was directly titrated with ethylenediaminetetraacetic acid (EDTA) disodium salt using murexide as the indicator. This gave the total amount of divalent cations in the sample. During titration, the pH value was adjusted to around 10 using diluted ammonia. At the end point, the color of the solution changed from yellow to violet. Potassium iodide (KI) was added to the second portion. The stoichiometric amount of iodine produced from the oxidation of I^- by trivalent cations (Co^{3+} and/or Fe^{3+}) in acidic solution was back-titrated with $Na_2S_2O_3$ using starch as the indicator. Because intercalated iodide and iodine may interfere with the KI titration, exchanged LDH samples in other anionic forms were also titrated using the same procedure to calibrate the results.

Results and Discussion

Reaction under Stoichiometric Iodine. As previously reported, $Co^{2+}_{2/3}Fe^{2+}_{1/3}(OH)_2$ (x = 1/3 in $Co^{2+}_{1-x}Fe^{2+}_{x}(OH)_2$) was transformed into I^--intercalated $Co^{2+}_{2/3}-Fe^{3+}_{1/3}$ LDH phase with a basal spacing of ∼8.3 Å using stoichiometric iodine for a treatment period of 12 h. The XRD pattern for the converted product is shown as "trace a" in Figure 1. However, when the same treatment with stoichiometric iodine was applied to $Co^{2+}_{3/4}Fe^{2+}_{1/4}(OH)_2$ and $Co^{2+}_{4/5}Fe^{2+}_{1/5}(OH)_2$ (x = 1/4 and 1/5 in $Co^{2+}_{1-x}Fe^{2+}_{x}(OH)_2$), mixed-layer products were instead obtained. A new basal spacing of ∼12.9 Å was yielded. This new spacing corresponds to the alternate stacking of I^--intercalated slab (8.3 Å) and residual brucite-like slab (4.6 Å), indicating the occurrence of second staging.[18] The residue of brucite-like slabs/components in the transformed product, even after a longer treatment period of 1 week, indicates incomplete conversion into a single LDH phase under stoichiometric iodine.

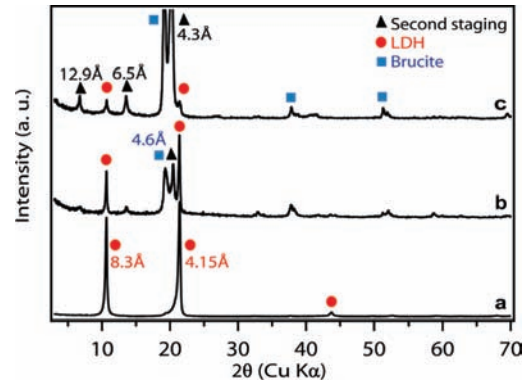

Figure 1. Mixed-layer products obtained after treating (a) $Co^{2+}_{2/3}Fe^{2+}_{1/3}(OH)_2$, (b) $Co^{2+}_{3/4}Fe^{2+}_{1/4}(OH)_2$, and (c) $Co^{2+}_{4/5}Fe^{2+}_{1/5}(OH)_2$ with stoichiometric iodine. In addition to I^--intercalated LDH (8.3 Å), residual brucite (4.6 Å) and the resultant second-staging structure (12.9 Å) were observed in products derived from the Fe/Co ratio lower than 1/2.

As Fe^{2+} is more easily to be oxidized than Co^{2+} in brucite hydroxide,[19] the transformation of $Co^{2+}_{1-x}Fe^{2+}_{x}(OH)_2$ under stoichiometric iodine may be considered as the sole oxidation of Fe^{2+} into Fe^{3+} by losing electrons to I_2 and simultaneous intercalation of in situ produced I^-. The reaction can be generally expressed as

$$Co^{2+}_{1-x}Fe^{2+}_{x}(OH)_2 + x/2I_2 \rightarrow Co^{2+}_{1-x}Fe^{3+}_{x}(OH)_2I_x$$

The above results thus demonstrate that, except for $Co_{2/3}Fe_{1/3}(OH)_2$ (x = 1/3), the standard oxidative intercalation synthesis cannot produce a single phase of LDH with Fe^{3+}/Co^{2+} ratio lower than 1/2 (i.e., x < 1/3) under the use of stoichiometric iodine ($x/2$ mol).

Reaction under Excess Iodine. Our earlier study indicates that the oxidation of Co^{2+} in brucite-like $Co(OH)_2$ by stoichiometric iodine was almost negligible despite that the oxidation potential of I_2/I^- (−0.535 V) is more negative than that of $Co(OH)_3/Co(OH)_2$ (−0.17 V).[12,19] A more oxidative agent, bromine, was used to oxidize Co^{2+} into Co^{3+} (the standard oxidation potential of Br_2/Br^- is −1.065 V). To ensure a complete conversion into a single $Co^{2+}-Co^{3+}$ LDH phase, the oxidative intercalation typically required as much as 40 times the amount of Br_2 and a long treatment duration of ∼5 days. Referring to the case of $Co^{2+}_{2/3}-Co^{3+}_{1/3}$ LDH obtained by excess bromine, a different amount of iodine, e.g., 1 × $x/3$ to 25 × $x/3$ mol, was employed to investigate the reactivity with brucite-like $Co^{2+}_{1-x}Fe^{2+}_{x}(OH)_2$ (x = 0, 1/5, 1/4, 1/3).

(17) Izumi, F.; Ikeda, T. *Mater. Sci. Forum* **2000**, *321−324*, 198.

(18) (a) Brindley, G. W.; Kikkawa, S. *Am. Mineral.* **1979**, *64*, 836. (b) Iyi, N.; Kurashima, K.; Fujita, T. *Chem. Mater.* **2002**, *14*, 583. (c) Iyi, N.; Fujii, K.; Okamoto, K.; Sasaki, T. *Appl. Clay. Sci.* **2007**, *35*, 218.

(19) Latimer, W. M. *Oxidation Potentials*, 2nd ed.; Prentice-Hall, Academic Press: Englewood Cliffs, NJ, and New York, NY, U.S., 1952.

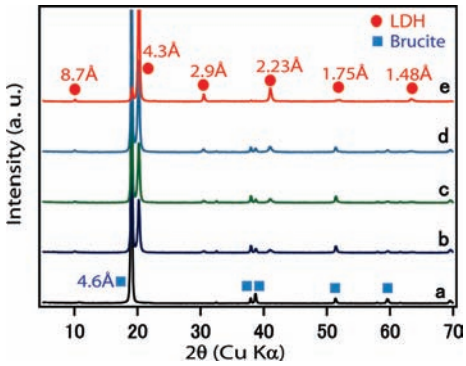

Figure 2. XRD patterns of products after reacting $Co(OH)_2$ with different amounts of iodine for different time periods: (a) stoichiometric (1/3 mol), 24 h; (b) 2.5 times (2.5 × 1/3 mol), 24 h; (c) 10 times (10 × 1/3 mol), 24 h; (d) 25 times (25 × 1/3 mol), 24 h; (e) 25 times, 120 h.

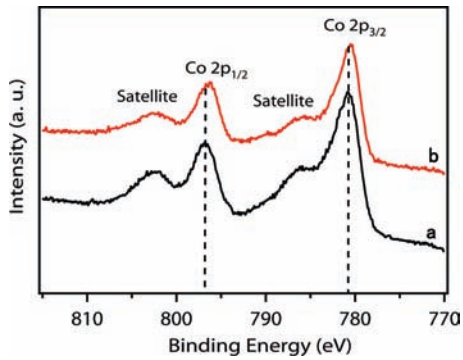

Figure 3. XPS of (a) brucite-like $Co(OH)_2$ and (b) layered phase of ~8.7 Å transformed under an excess amount of iodine.

Although there was no apparent change for $Co(OH)_2$ ($x = 0$ in $Co^{2+}_{1-x}Fe^{2+}_x(OH)_2$) under stoichiometric iodine (1 × 1/3 mol) as seen in "trace a" in Figure 2, it appeared that the brucite hydroxide gradually transformed into a new layered phase when reacted with an excess amount of iodine for a prolonged period. The transformation was manifested by XRD observations in which the basal peak at 4.6 Å for brucite-like $Co(OH)_2$ was weakened, whereas a new peak emerged at 4.3 Å. The reaction seems to be promoted with the increased amount of iodine (traces b−e). When an amount of 25 times iodine was used, the residual peak at 4.6 Å almost disappeared after a reaction time longer than 5 days. Instead, the peak at 4.3 Å became dominant. Almost all the new peaks can be indexed to a layered phase with a basal spacing of ~8.7 Å (first order, 8.7 Å; second, 4.3 Å; third, 2.9 Å; fourth, 2.23 Å; fifth, 1.75 Å; sixth, 1.48 Å), although the intensity of the first-order peak was abnormally low.

Typical XPS data of starting brucite-like $Co(OH)_2$ and as-transformed layered phase are compared in Figure 3. The Co 2p core lines of $Co(OH)_2$ are split into Co $2p_{3/2}$ (780.2 eV) and Co $2p_{1/2}$ (796.6 eV) main peaks accompanied by satellite bands at 785.5 and 802.1 eV, respectively. Prominent Co $2p_{3/2}$ satellite bands are indicative of a high-spin Co^{2+} state. After excess iodine treatment, the Co $2p_{3/2}$ and Co $2p_{1/2}$ main peaks slightly shift to lower energy regions, 779.7 and 795.5 eV, respectively. The intensity of the satellite bands also decreases to some degree. These spectroscopic differences suggest a partial valence change trend from Co^{2+} into Co^{3+}. This implies that the oxidation of Co^{2+} may be kinetically favored, e.g., a concentration effect under the condition of using excess iodine, and becomes possible under prolonged reaction duration. The

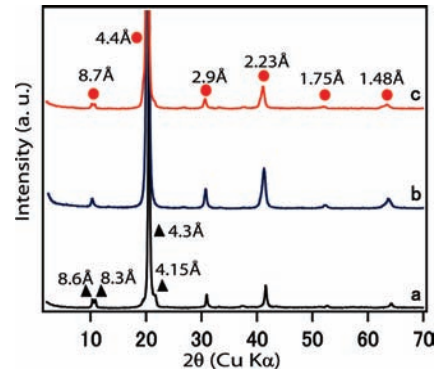

Figure 4. XRD patterns of products obtained by treating $Co^{2+}_{1-x}Fe^{2+}_x(OH)_2$ with excess iodine (>10 × x/2 mol) for 5 days, (a) $x = 1/3$; (b) $x = 1/4$, and (c) $x = 1/5$.

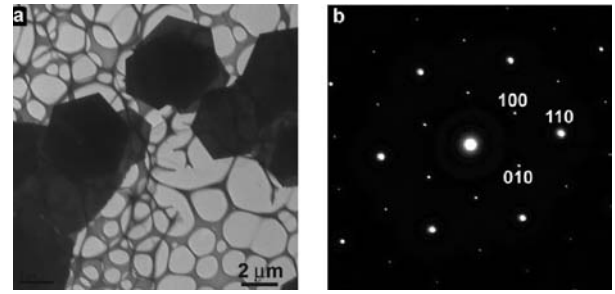

Figure 5. (a) TEM observation of products transformed from $Co_{3/4}Fe_{1/4}(OH)_2$ under excess iodine. (b) Typical electron diffraction pattern of individual platelet, exhibiting in-plane hexagonal symmetry.

transformed layered product with basal spacing of ~8.7 Å might be an LDH phase in mixed valences, i.e., $Co^{2+}-Co^{3+}$ LDH.

Similarly, when brucite-like $Co^{2+}_{1-x}Fe^{2+}_x(OH)_2$ at other Fe/Co ratios ($x = 1/5, 1/4, 1/3$) were treated by excess iodine (>10 × x/2 mol) for longer than 5 days, almost identical XRD patterns were obtained resembling that on $Co(OH)_2$ ($x = 0$), featured with a major peak at 4.3 Å and a much weaker first-order peak at 8.6−8.7 Å (Figure 4). All the peaks can be assigned to a layered phase with a basal spacing of ~8.7 Å. It is noteworthy that $Co_{2/3}Fe_{1/3}(OH)_2$ ($x = 1/3$) was also transformed into this layered phase after the reaction with excess iodine, despite that a minor phase with basal spacing of 8.3 Å coexisted. This is very different from the standard reaction of $Co_{2/3}Fe_{1/3}(OH)_2$ under stoichiometric iodine, which yielded a single phase of I^--intercalated $Co^{2+}_{2/3}-Fe^{3+}_{1/3}$ LDH (8.3 Å). Furthermore, for $Co^{2+}_{2/3}-Fe^{3+}_{1/3}$ LDH obtained by using stoichiometric iodine, the intensity of the first-order basal peak was somewhat lower than that of the second one (trace a in Figure 1), which could be explained by the intercalation of I^- with large X-ray scattering power. The unusual low intensity of the first basal peak for the ~8.7 Å layered phases obtained from excess iodine treatment suggests that another anionic species with much higher scattering power of X-ray than that of I^- might be introduced into the interlayer gallery, which causes the unusual intensity ratio of XRD peaks. This will be discussed later.

Microscopic observations revealed that as-transformed products under excess iodine consisted of hexagonal platelets with a lateral size of 2−4 μm and thickness of several tens of nanometers, resembling the size and shape of starting brucite-like hydroxides.[12,13] For example, Figure 5 displays a TEM image of the product transformed from $Co_{3/4}Fe_{1/4}(OH)_2$. The

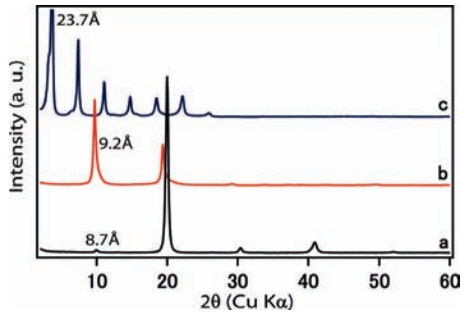

Figure 6. Evolution of XRD patterns during anion exchange. (a) As-transformed product obtained by reacting $Co_{3/4}Fe_{1/4}(OH)_2$ with excess iodine. (b) Exchanged product with perchlorate (ClO_4^-) and (c) dodecyl sulfate ($C_{12}H_{25}OSO_3^-$).

typical electron diffraction pattern on an individual platelet, exhibiting in-plane hexagonal symmetry $a = 3.1$ Å, verifies the single crystallinity of as-transformed products. The morphological preservation supports the topotactic nature of the oxidative intercalation reaction even though excess iodine was employed.

The ∼8.7 Å layered phase can be exchanged for a variety of anions ranging from inorganic to organic species, such as perchlorate and dodecyl sulfate (DS, $C_{12}H_{25}OSO_3^-$). As seen in Figure 6, the evolution of XRD patterns during anion exchange indicates that the products are of single-phase purity. For example, interlayer spacing values of the exchanged products intercalating ClO_4^- (9.2 Å) and DS (23.7 Å) are consistent with the documented data on LDHs.[12−14] The striking contrast before and after exchange lies in the intensity ratio between the first-order and second-order peaks in the XRD patterns. The as-transformed layered product obtained by oxidative intercalation exhibited a dominant peak at 4.3 Å whereas a much weaker first-order peak appears at ∼8.7 Å. After anion exchange into either ClO_4^- or DS form, the intensity ratio reversed to a normal profile with a stronger first-order peak as typically observed in common layered compounds. The reversal in intensity ratio provides a meaningful clue in that a peculiar interlayer anionic species, incorporated during the oxidative intercalation process, may account for the abnormal XRD patterns observed in as-transformed ∼8.7 Å layered products.

Figure 7 displays TG curves of as-transformed product obtained from $Co_{3/4}Fe_{1/4}(OH)_2$ under excess iodine in comparison with those of normal I^--intercalated $Co^{2+}_{2/3}-Fe^{3+}_{1/3}$ LDH. It is obvious that as-transformed ∼8.7 Å product gave a much higher weight loss, ∼50%, compared to ∼34% for I^--intercalated $Co^{2+}_{2/3}-Fe^{3+}_{1/3}$ LDH. After the exchange into other anionic forms, e.g., ClO_4^-, almost the same weight loss profile with normal ClO_4^--intercalated $Co^{2+}_{2/3}-Fe^{3+}_{1/3}$ LDH was

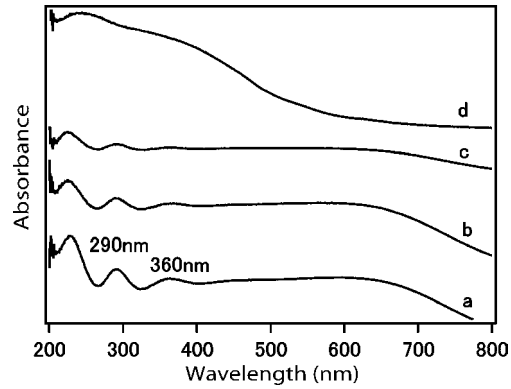

Figure 8. UV−vis absorption spectra of as-transformed ∼8.7 Å layered products after treating $Co^{2+}_{1-x}Fe^{2+}_x(OH)_2$ (a) $x = 1/3$, (b) $x = 1/4$, and (c) $x = 1/5$ with excess iodine treatment. (d) Exchanged product in DS form. The common band near ∼230 nm is possibly due to charge transfer between cobalt and oxygen.

observed. This offers strong evidence that the product transformed by excess iodine is a layered phase very similar to conventional LDHs except for the intercalation of a higher content of iodine in the gallery. Elemental analyses of the samples in TEM showed that the average molar ratio of iodine in the transformed products was ∼1.6 times that in normal I^--intercalated $Co^{2+}_{2/3}$-$Fe^{3+}_{1/3}$ LDH (approximately 1/3 per chemical formula). This results in average iodine content per chemical formula at $1.6 \times 1/3$.

It is well-known that iodide may bind with iodine to form triiodide in a concentrated iodine/iodide solution:

$$I_2 + I^- \rightarrow I_3^-$$

A number of one-electron redox reactions can occur in the iodide−iodine system, which makes the iodide/triiodide couple useful as an effective redox mediator, e.g., in dye-sensitized solar cells.[20] The high content of iodine in the samples reacted with excess iodine, confirmed by both elemental analysis and TG data, points to the possibility that a new anionic species, I_3^-, might be incorporated into the gallery of the ∼8.7 Å layered phase.

UV−vis absorption spectra of as-transformed ∼8.7 Å layered products are shown in Figure 8. Two absorption maxima at 290 and 360 nm may be assigned to I_3^-, corresponding to the spin- and symmetry-allowed $\sigma \rightarrow \sigma^*$ and $\pi \rightarrow \sigma^*$ transitions.[21] On the other hand, spin-forbidden singlet−triplet transitions of I_3^-, expected at 440 and 560 nm, which may be significantly enhanced if I_3^- is in a low symmetry, are not observed. The spectroscopic features thus support the intercalation of linear

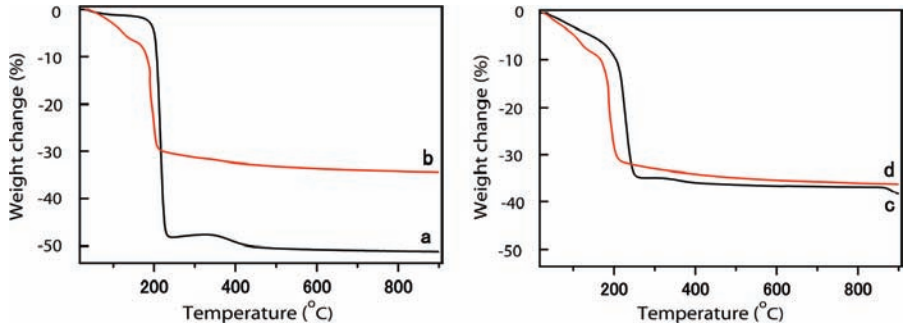

Figure 7. TG curves of (a) as-transformed product obtained by reacting $Co_{3/4}Fe_{1/4}(OH)_2$ with excess iodine and (b) its exchanged form containing ClO_4^-; (c) I^--intercalated $Co^{2+}_{2/3}-Fe^{3+}_{1/3}$ LDH and (d) exchanged $Co^{2+}_{2/3}-Fe^{3+}_{1/3}$ LDH containing ClO_4^- for reference.

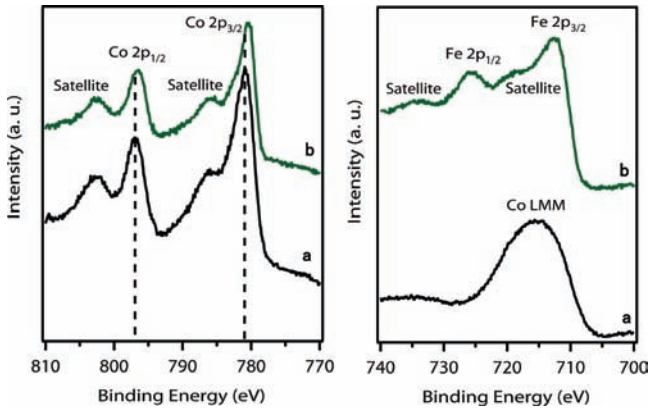

Figure 9. XPS measurements of Co (left panel) and Fe (right panel) valence states in (a) brucite-like $Co(OH)_2$ and (b) as-transformed LDH product from $Co^{2+}_{4/5}Fe^{2+}_{1/5}(OH)_2$ using excess iodine. The spectroscopic results indicate a possible Fe^{3+} state and some Co^{3+} components in the as-transformed LDH product.

triiodide between the layers. Furthermore, both bands related to I_3^- disappeared after the anion exchange into DS form. Therefore, interlayer triiodide in the products was readily exchangeable.

As ferrous cations within the brucite layers can be easily oxidized to Fe^{3+} by iodine, it is reasonable to deduce that all Fe^{2+} in brucite $Co^{2+}_{1-x}Fe^{2+}_x(OH)_2$ ($x = 1/5, 1/4, 1/3$) would be oxidized to a trivalent state. For example, the XPS spectrum on as-transformed product from $Co^{2+}_{4/5}Fe^{2+}_{1/5}(OH)_2$ using excess iodine is given in Figure 9. The overlap from the Co LMM Auger peak near 715 eV increases the difficulty of analyzing the exact valence. Nevertheless, the appearance of satellite bands near the Fe 2p main peaks is generally regarded as an indicator of Fe^{3+} valence state. Similarly, a clear determination of oxidation state for cobalt is also difficult as the Fe LMM Auger peak near 785 eV overlaps the energy region for the Co core lines. However, the slight shift of main peaks to lower energy levels and the decrease in intensity of the satellite bands, in comparison with that of brucite-like $Co(OH)_2$, might be caused by some possible Co^{3+} components in the I_3^--intercalated product. Based on the aforementioned experimental observations on brucite-like $Co(OH)_2$ verifying the feasibility of partial oxidation of Co^{2+} to Co^{3+} using excess iodine, it may be reasonable to speculate that a similar oxidation of Co^{2+} to Co^{3+} in $Co^{2+}_{1-x}Fe^{2+}_x(OH)_2$ is also plausible. Wet chemical analyses determined that the molar ratio of total trivalent and divalent cations in all as-transformed layered phases was close to 1/2 regardless of Fe/Co ratio. This also supports that some Co^{2+} may be oxidized to the trivalent state if the Fe^{3+} content alone cannot reach the 1/2 threshold, e.g., in $Co^{2+}_{4/5}Fe^{2+}_{1/5}(OH)_2$ or $Co^{2+}_{3/4}Fe^{2+}_{1/4}(OH)_2$. Combined with the EDS analysis on iodine, the compositions were estimated as $Co^{2+}_{2/3}(Co^{3+}_{1/12}Fe^{3+}_{1/4})(OH)_2I_{0.54}\cdot 0.2H_2O$, $Co^{2+}_{2/3}(Co^{3+}_{2/15}Fe^{3+}_{1/5})(OH)_2I_{0.51}\cdot 0.2H_2O$, and $Co^{2+}_{2/3}Fe^{3+}_{1/3}(OH)_2I_{0.49}\cdot 0.2H_2O$, respectively.

Structure Model and XRD Simulation. The determination of LDH structure involves both the cation arrangement in the host layer, which controls the charge distribution, and the corresponding anion distribution in the interlayer gallery. If the rule for avoidance of nearest neighboring M^{3+} charge centers is strictly followed, long-range ordering will produce possible two-dimensional supercells in the host layers. The dimension of a supercell is closely related to the layer charge ($M^{3+}/(M^{2+} + M^{3+})$). For example, a schematic model shown in Figure 10

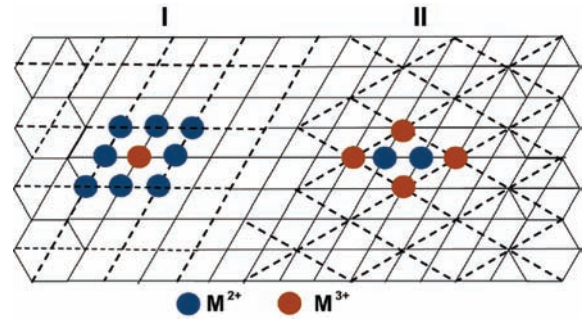

Figure 10. Possible cation ordering in the host layer for different M^{3+}/M^{2+} ratios. The solid parallelogram represents the primary unit cell. The length of cell edges is a: cation−cation distance. (I) $2a \times 2a$ supercell structure in $M^{3+}/M^{2+} = 1/3$; (II) $\sqrt{3}a \times \sqrt{3}a$ supercell in $M^{3+}/M^{2+} = 1/2$. Each supercell (dotted parallelogram) contains one positive charge.

depicts the possible arrangement of metal cations in the host layer derived from $Co^{2+}_{3/4}Fe^{2+}_{1/4}(OH)_2$. If only Fe^{2+} is being oxidized, a layer charge ($[Co^{2+}_{3/4}Fe^{3+}_{1/4}(OH)_2]^{1/4+}$) would be attained. Supercell $2a \times 2a$ (a: cation−cation distance), containing three M^{2+} and one M^{3+} ($M^{3+}/M^{2+} = 1/3$) for one positive charge, comes into being in the host layer. On the other hand, if the oxidation of both Co^{2+} and Fe^{2+} is possible, a higher layer charge ($[Co^{2+}_{2/3}(Co^{3+}_{1/12}Fe^{3+}_{1/4})(OH)_2]^{1/3+}$) may be yielded. In this case, each supercell contains one positive charge associated with two M^{2+} and one M^{3+} ($M^{3+}/M^{2+} = 1/2$) in cell dimensions of $\sqrt{3}a \times \sqrt{3}a$.

Each supercell, in dimensions of either $2a \times 2a$ or $\sqrt{3}a \times \sqrt{3}a$, will produce one anionic site in the interlayer gallery. Each anion will share its charge with one M^{3+} cation in the layer underneath and one in the layer above. There are six equivalent sites surrounding each anionic site, comprising a hexagonal arrangement of anions. Figures 11 and 12 illustrate the possible distribution of interlayer iodide. The ionic diameter of I^- (4.32 Å)[22] is much larger than the cation−cation distance of ~3.1 Å. Each supercell will be charge-balanced by a spherical iodide, separated by a distance of $2a$ (6.20 Å) or $\sqrt{3}a$ (5.37 Å) and commensurate with the cationic ordering in the host layer.

For layer charge $1/4^+$ ($2a \times 2a$ supercell), if each available anionic site is occupied by I^-, a model composition of $Co^{2+}_{3/4}Fe^{2+}_{1/4}(OH)_2I_{1/4}\cdot 0.2H_2O$ (i.e., iodine content per formula: $I_{0.25}$) is obtained. The iodine content is apparently lower than the analyzed value. Figure 11b shows the simulated low-angle XRD pattern using this estimated chemical formula. The first-order basal reflection has a higher intensity than the second-order one and is obviously different from those observed experimentally. The XRD pattern profile changes dramatically by considering the occupation of linear I_3^- at available anionic sites, which has a much higher X-ray scattering power. The dimensions of linear triiodide are estimated to be 4.32 × 9.64 Å².[23] Taking the steric factor into account, one-third of the available anionic positions ($Co^{2+}_{3/4}Fe^{3+}_{1/4}(OH)_2(2/3I + 1/3I_3)_{1/4}$ (i.e., iodine content per formula: $I_{0.42}$) to as high as half ($Co^{2+}_{3/4}$-

(20) Boschloo, G.; Hagfeldt, A. *Acc. Chem. Res.* **2009**, *42*, 1819.
(21) (a) Gabes, W.; Stufkens, D. J. *Spectrochim. Acta: Part A: Mol. Biomol. Spectrosc.* **1974**, *A 30*, 1835. (b) Howard, W. F.; Andrews, L. *J. Am. Chem. Soc.* **1975**, *97*, 2956. (c) Mohanambe, L.; Vasudevan, S. *Inorg. Chem.* **2004**, *43*, 6421.
(22) Shannon, R. D.; Prewitt, C. T. *Acta Crystallogr.* **1969**, *B25*, 925.
(23) Covalent bonding radius and ionic radius of iodine is 1.33 and 2.16 Å, respectively. The length of linear I_3^- may be calculated as 2.16 × 2 + 1.33 × 4 = 9.64 Å.

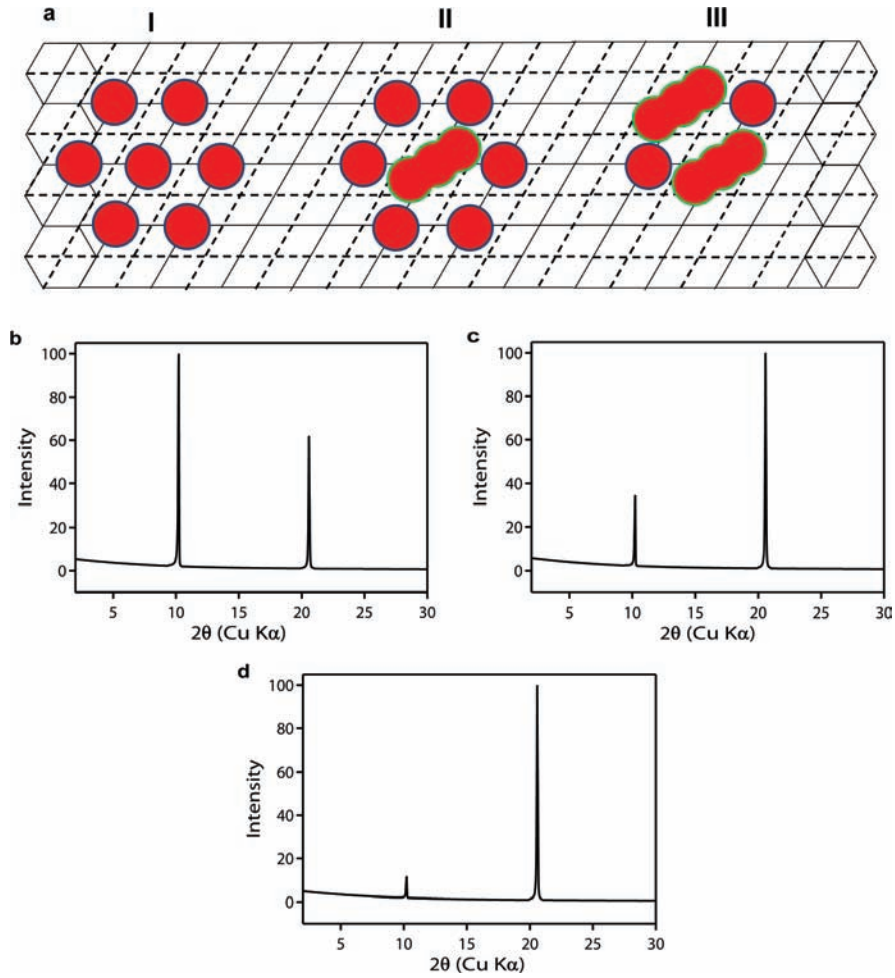

Figure 11. (a) Possible distribution of interlayer iodide and triiodide for $M^{3+}/M^{2+} = 1/3$ ($2a \times 2a$ supercell). Charge balance produces one available anionic site (I^- or I_3^-) for each supercell (dotted parallelogram). (I) $1/4I^-$; (II) $1/4\ (2/3I^- + 1/3I_3^-)$; (III) $1/4\ (1/2I^- + 1/2I_3^-)$. (b, c, d) Simulated low-angle XRD patterns for interlayer anion content corresponding to (I) $1/4I^-$; (II) $1/4\ (2/3I^- + 1/3I_3^-)$, and (III) $1/4\ (1/2I^- + 1/2I_3^-)$, respectively.

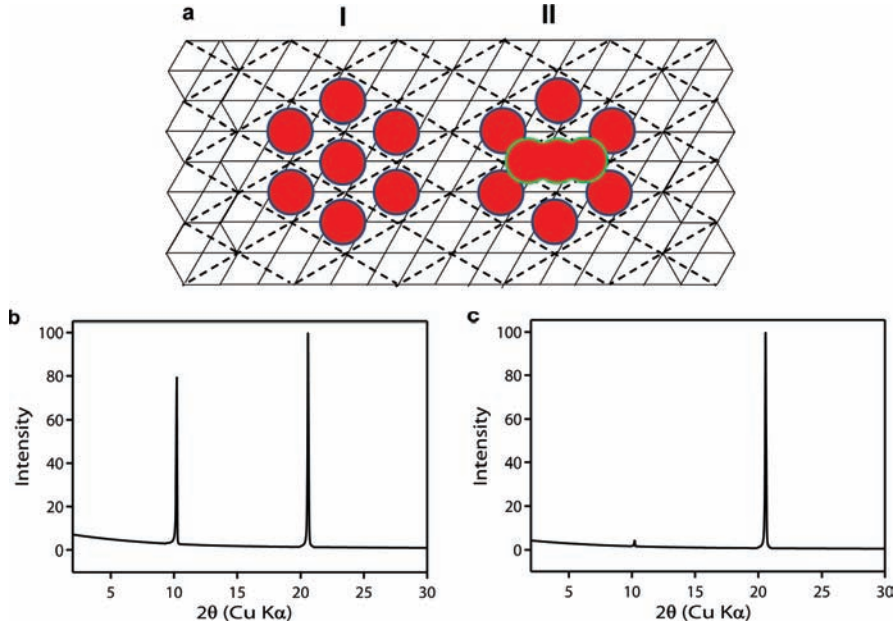

Figure 12. (a) Possible distribution of interlayer iodide and triiodide for $M^{3+}/M^{2+} = 1/2$ ($\sqrt{3}a \times \sqrt{3}a$ supercell). Charge balance produces one available anionic site (I^- or I_3^-) for each supercell (dotted parallelogram). (I) $1/3I^-$; (II) $1/3\ (2/3I^- + 1/3I_3^-)$. (b, c) Simulated low-angle XRD patterns for interlayer anion content corresponding to (I) $1/3I^-$ and (II) $1/3\ (2/3I^- + 1/3I_3^-)$, respectively.

$Fe^{3+}_{1/4}(OH)_2(1/2I + 1/2I_3)_{1/4}$ (i.e., iodine content per formula: $I_{0.50}$) might be occupied by triiodide. According to the simulations, the first-order basal reflection becomes much weaker than the second-order one via the intercalation of one-third iodide (Figure 11c). When half the available anionic positions are occupied by triiodide (Figure 11d), the iodine content is close to the analysis result and a relatively good fit to the experimental data is noted, but the first peak still appears somewhat high in intensity.

As illustrated in Figure 12a, when the layer charge is increased to $1/3^+$, i.e., $\sqrt{3}a \times \sqrt{3}a$ supercell in the host lattice, the rate of iodide occupancy will also be increased to 1/3 if it is assumed that only simple iodide is intercalated. The XRD simulation produces the pattern shown in Figure 12b, in which the first-order basal reflection is somewhat lower than the second-order one, which is consistent with the observation on $Co^{2+}_{2/3}-Fe^{3+}_{1/3}$ LDH ("trace a" in Figure 1).[12] The peak ratio is quite different from the experimental value in the current study. This again proves that the observed XRD patterns cannot be explained as a sole intercalation of iodide. When triiodide is cointercalated, steric consideration given in Figure 12a indicates that, at most, one-third of the available anionic sites may be occupied by triiodide. A total interlayer anion content of 1/3(2/3I + 1/3I_3), i.e., iodine content $I_{0.555}$ per formula, may be yielded. The iodine content is very close to the chemical analysis data. Simulated XRD pattern in this model is characteristic of negligible first-order basal reflection in comparison with a dominant second-order one, which fits well with the experimental result.

As the XRD patterns are predominantly affected by the interlayer iodine content, the above model description and XRD simulation are applicable to transformed LDH products in other Fe/Co ratios. General $Co^{2+}_{2/3}-(Co^{3+}_{1/3-x}-Fe^{3+}_x)$ LDHs, regardless of Fe/Co ratio, exhibit the same M^{3+}/M^{2+} ratio of 1/2 and total interlayer anion content close to 1/3(2/3I + 1/3I_3). This actually well explains why almost identical XRD patterns were obtained for all the ~8.7 Å LDH products derived from $Co^{2+}_{1-x}Fe^{2+}_x(OH)_2$ under the treatment of excess iodine. We speculate that the cointercalation of triiodide may slightly prop up the gallery compared to the intercalation of iodide alone to increase the basal spacing from 8.3 to 8.7 Å. It is noteworthy that a coexisting minor phase with basal spacing of 8.3 Å is observed in the product transformed from $Co^{2+}_{2/3}Fe^{2+}_{1/3}(OH)_2$. A normal I^--intercalated $Co^{2+}_{2/3}-Fe^{3+}_{1/3}$ LDH can be formed in this sample through the oxidation of ferrous cations solely at a rapid rate without the need to partially oxidize Co^{2+} into Co^{3+}. This might infer that the intercalation of I_3^- was not kinetically prompted in the reaction. Though triiodide still might be intercalated or exchanged into the gallery, an amount slightly less than that in other samples may account for the 8.3 Å minor phase.

It needs to be noticed that the above discussion and simulation are based on an ideal model, $\sqrt{3}a \times \sqrt{3}a$ supercell, assuming that direct nearest neighboring of charge centers (Fe^{3+} or Co^{3+}) is unfavorable. In fact, if Co^{2+} and Fe^{2+} are homogeneously distributed in brucite $Co^{2+}_{3/4}Fe^{2+}_{1/4}(OH)_2$ and $Co^{2+}_{4/5}Fe^{2+}_{1/5}(OH)_2$ following the designed molar ratio, it means an initial ordering or superlattice of Fe^{2+} in the host layer may be already predetermined, e.g., $2a \times 2a$ ordering in $Co^{2+}_{3/4}Fe^{2+}_{1/4}(OH)_2$. The total oxidation of all Fe^{2+} to Fe^{3+}, together with the partial oxidation of Co^{2+} to Co^{3+}, will inevitably result in direct nearest neighboring of Fe^{3+} and Co^{3+}. The formation of ideal $\sqrt{3}a \times \sqrt{3}a$ supercells in resultant LDH is therefore not as straightforward as illustrated in Figure 10. The cation arrangement of Fe^{3+} and Co^{3+} may be more complicated than the ideal case. The possibility even exists that local charge hopping occurs among neighboring Fe^{3+}, Co^{3+}, and Co^{2+}. Nevertheless, the basis for discussion is valid for all Fe/Co ratios in terms of the interlayer iodide and triiodide content, which is commensurate in charge balance with the 1/2 molar ratio of total trivalent and divalent cations in the host layer. Further investigation into the exact and detailed cation distribution in $Co^{2+}-(Co^{3+})-Fe^{3+}$ LDHs at different Fe/Co ratios would be interesting. Such a study may also correlate and provide the rationale for the formation of in-plane two-dimensional superlattices in other layered materials, e.g., lithium insertion layered transition metal oxides such as $LiCoO_2-LiNiO_2-LiMnO_2$[24] as well as $Fe^{2+}-Fe^{3+}$ hydroxysalt green rusts.[25] It is also worth adding that, except for coprecipitation where it seems possible to produce LDHs in M^{3+}/M^{2+} ratios other than 1/2, the oxidative intercalation procedure, analogous to homogeneous precipitation, would only yield host layer compositions in 1/2 molar ratio of total trivalent and divalent cations. The reason for this intriguing phenomenon might stem from the fact that the latter two methods equilibrate more thermodynamically than coprecipitation. This awaits further investigations.

Conclusion

Co−Fe LDHs were synthesized from brucite-like $Co^{2+}_{1-x}Fe^{2+}_x(OH)_2$ ($0 \le x \le 1/3$) via an oxidative intercalation reaction using an excess amount of iodine as the oxidizing agent. The experimental characterization, structural model discussion, and XRD simulation revealed two important facts associated with the peculiar procedure. First, the molar ratio of total trivalent and divalent cations in all transformed LDHs is close to 1/2 regardless of Fe/Co ratio. This correlates with previous observations on $Co^{2+}_{2/3}-Co^{3+}_{1/3}$ and $(Co^{2+}_{1-3x/2}-Ni^{2+}_{3x/2})_{2/3}-Co^{3+}_{1/3}$ LDHs and may be regarded as a general principle governing the oxidative intercalation. Excess iodine used as the oxidizing agent helped to produce a single pure phase of Co−Fe LDHs through partial oxidation of Co^{2+} to Co^{3+} when Fe^{3+} content was low, e.g., $Co^{2+}_{1-x}Fe^{2+}_x(OH)_2$ ($x < 1/3$). Second, cointercalation of triiodide generated from concentrated iodine solution, which is rather rare to obtain through normal anion exchange, provided unique insight into the oxidative intercalation reaction regarding host layer composition and cation ordering, as well as interlayer anion species and steric distribution. The principle and experimental discoveries are helpful in interpreting the formation of LDH structure in general and serve well in understanding other related synthetic methods such as coprecipitation and homogeneous precipitation.

Acknowledgment. This work was supported by the World Premier International Research Center (WPI) Initiative on Materials Nanoarchitectonics of MEXT, and CREST of Japan Science and Technology Agency, Japan.

JA1087216

(24) Koyama, Y.; Makimura, Y.; Tanaka, I.; Adachi, H.; Ohzuku, T. *J. Electrochem. Soc.* **2004**, *151*, A1499.
(25) Génin, J.-M. R.; Ruby, C. *Solid State Sci.* **2004**, *6*, 705.